Development of a High Strain-Rate and Temperature Impact Bench

Miguel E. L. Saragoça
miguel.saragoca@tecnico.ulisboa.pt
Instituto Superior Técnico, Universidade de Lisboa, Portugal
January 2021

Abstract

The development of new materials always marks a technological leap, as their use promotes the development of new equipment and an improvement in the performance of existing technologies. This evolution poses new challenges for mechanical testing laboratories in the characterization of the mechanical behaviour of high-strength materials and the evaluation of the performance of components under conditions representative of industrial, civil or military applications.

The present work seeks the development of a testing machine that allows uniaxial compression of materials under conditions of high strain-rate and high temperature.

The validation of the equipment was based on the reproduction of case studies available in the literature, and later the equipment was used for the mechanical characterization of metal alloys recently used for additive manufacturing, focusing on maraging steel, grade 300, produced by Selective Laser Melting (SLM).

Keywords: mechanical characterization, uniaxial compression, impact, maraging.

1. Introduction

The study of the characteristics and mechanical behaviour of materials when subjected to external loads is of fundamental importance for our life. On the one hand, from the point of view of application, at the structural level for example, the choice of a material over another is conditioned by characteristics that are both intrinsic, such as the modulus of elasticity, and extrinsic, such as load, which affect its behaviour. On the other hand, from a fundamental point of view, the material behaviour characterization, through mechanical tests and the design and validation of constitutive models based on these, allows a better knowledge of their response, something of special importance when introducing new manufacturing techniques or new materials, for which the response to external efforts is not yet fully known.

The parameters for the empirical constitutive models that describe the influence of the operating conditions, be it the temperature or the strain-rate, can be obtained experimentally from the stress-strain curve of the material. There is a lack of information on the mechanical behaviour of materials for high strains at high strain-rates, and even less information for the combined effects of high strain-rates and high temperature conditions [1], so the development of testing equipment, such as the one developed in this work, that are able to replicate a wide range of loads, deformation speeds and temperatures, is of utmost importance.

2. Theoretical Background

Mechanical Behaviour

The behaviour of materials is diverse, and can be rationalized through the characterization of the stress-strain curve. In general, the material's response to external loads, exhibits both elastic and plastic behaviour. The simplicity of elastic behaviour, in the form of a linear relationship between stress and strain

$$\sigma = E\,\varepsilon \tag{1}$$

is not valid in the general case of plastic deformation. In this case, the non-linearity of the stress-strain relationship itself imposes a commensurably greater effort in the development of the constitutive model that determines it. In metals, this non-linearity appears as an effect of complex and the stochastic characteristic of the mechanisms behind plastic deformation processes, such as dislocation mobility or

migration of grain boundaries [2], or, for example, of work hardening processes, related to the density of dislocations.

In addition, the viscous effects cause the mechanical response of the materials to depend on the speed at which the deformation is applied [3]. Furthermore, materials that are ductile at room temperature typically become even more ductile at higher temperatures, and at lower temperatures they may become brittle. Thus, when considering the temperature in characterizing the behaviour of materials under external loads, the stress-strain curves become even less linear [4].

Constitutive Models

The characterization of the mechanical behaviour of the materials can be done through constitutive models. The visco-plastic models also account for the effects of temperature and deformation speed, these parameters being the focus of the present work. The hybrid empirical constitutive models allow, through a single constitutive equation, to reproduce several traditional models.

The Johnson-Cook model [5] is one of the most widely used visco-plastic models. It contemplates the effects of temperature and strain rate and is suitable for modelling the material behaviour over a wide range of strain rates. This model's equation

$$\sigma = (A + B\varepsilon^n)\left(1 + \ln\left(\frac{\dot{\varepsilon}}{\dot{\varepsilon}_0}\right)^m\right)\left(1 - \left(\frac{T - T_r}{T_f - T_r}\right)^p\right) \quad (2)$$

can be separated into three parts, the first directly related to hardening effects, the second related to the deformation speed and the third related to thermal effects.

Silva's model [6] is an empirical visco-plastic model proposed for the mechanical behaviour of cold materials, given by the expression:

$$\sigma = [A + e^{m\varepsilon}\varepsilon^n][B + C\ ln(D + \dot{\varepsilon})] \quad (3)$$

Where A, B, C, D, m and n are constants that depend on the material and can be determined experimentally. An adaptation of this model will be used in this work to attempt model the tested materials behaviour, adding another term, based on the last part of the Johnson-Cook's equation, that encompasses the temperature effects.

Uniaxial Compression Test

The present work is based on the uniaxial compression test in order to determine the characteristic stress-strain curve of the materials under different conditions of temperature and strain-rate. It consists of subjecting a cylindrical specimen to a compressive force, recording the force measured for each increment of displacement.

The true stress and strain can be obtained by the following expressions:

$$\sigma = \frac{F}{A_i} \quad (4)$$

$$\varepsilon = -\int_{h_0}^{h_i} \frac{dh}{h} = \ln\frac{h_0}{h_i} \quad (5)$$

where F is the measured force, h_0 is the initial specimen's height and h_i and A_i are the height and cross sectional area of the specimen at any given instance of the compression.

One of the equipment often used to perform compression tests at high strain rates, around 5000 s^{-1}, is the Split-Hopkinson Pressure Bar (SHPB). Figure 1 shows the typical scheme of this type of equipment. A projectile, accelerated using a propulsion system, collides with an incident bar, creating an elastic pressure wave that travels through it. A part of this wave is transmitted to the specimen and consequently to the transmitter bar, the other part being reflected back to the incident bar. The installation of strain gauges on the bars allows the monitoring of these pressure waves and, through mathematical relationships, it is possible to determine the stress-strain curve of the material [7].

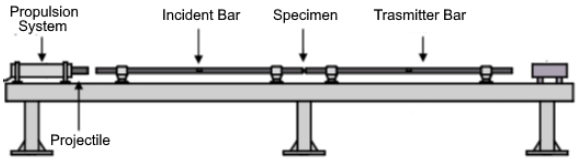

Figure 1 - Scheme of a typical Split-Hokinson Pressure Bar apparatus [8].

3. Experimental Development

The experimental apparatus developed in this work is based on the SHPB model, but, unlike this model, only the transmitter bar will be instrumented with a strain gauge and the instantaneous height of the specimen registered, thus resembling a conventional compressive testing equipment.

The Main Structure

The pre-existing structure present in the laboratory, developed in the studies of Pedro Monteiro (2007) and José Pinto (2009), consisted of three support columns and an I-beam. This structure, however, had a low structural stiffness that could be observed by the flexing of the beam under high load quasi-static compressive tests. This problem was solved by fixing the three columns to the floor, in order to create a closed structural frame, and by welding two U-beams between the columns, to further reinforce this frame.

To this reinforced base structure, it is now possible to attach all the equipment necessary for carrying out the compression tests. An additional support structure was developed, attached to the base structure, that holds the incident and transmitter bars. Manufactured in 20 mm thick AISI 1045 steel plates, as seen in figure 2, this structure is characterized by a high rigidity and an absence of any slack in the fasteners, characteristics that allow compression tests in demanding conditions without compromising the quality of the results.

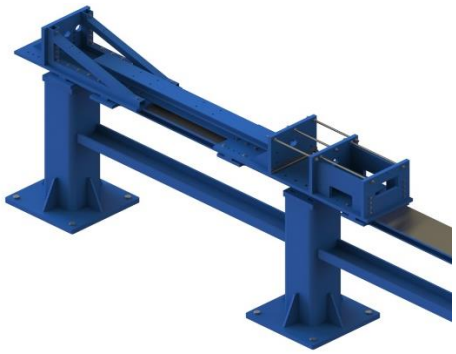

Figure 2 - Support structure for the bars attached to the base structure.

Incident and Transmitter Bar

Titanium alloy (Ti6Al4V) rods were used for the incident and transmitter bars. With this material it was possible to have bars with a greater mechanical strength; this alloy's compressive yield stress of 970 MPa guarantees the permanence in the elastic region during the tests with high loads, up to a maximum of 87.3 kN.

The two titanium bars, with a length of 500 mm for the incident bar, 1500 mm for the transmitter and an identical diameter of 30 mm must be aligned concentrically and move longitudinally with the least possible friction. In order to fulfil these two requirements, linear ball bearings were installed, which support the bars, and allow the adjustment of their alignment, as well as allowing a longitudinal movement with low friction (Coefficient of Friction (COF) = 0.001), provided a correct lubrication.

The severe conditions observed in the compression zone of the specimen, such as high impact speeds and high temperatures, led to the installation of compression rods, whose ends work as compression plates, produced in a material tougher than titanium. Tungsten carbide rods in a cobalt matrix (WC-Co10%) with 18 mm of diameter were used, manufactured using wire EDM and surface grinding, in order to guarantee the flatness between their surfaces. These compression rods were fixed to one end of each titanium bar by mechanical interference: the hole in the titanium bars whose diameter was, at room temperature, slightly smaller than the diameter of the rods, was expanded by heating. The expansion allowed the rods to be introduced and, after cooling, ensured a solid clamping and fastening.

One of the problems found in preliminary tests was the premature breaking of these rods, especially when impact tests were performed on titanium alloy specimens. The specimen tended to adhere to the surface of the rods, causing them to rupture. In a first analysis of this problem, the failure mechanism could be related to the friction between the specimen surfaces and the carbide rods. The polishing of the compression surfaces of the rods and the use of graphite-based lubricant allowed better results, except in titanium alloy specimens.

In this particular case, the adhesion of surfaces is explained by the affinity between the titanium of the specimen and the cobalt of the tungsten carbide matrix. This situation, which typically occurs when machining titanium with inserts of this type, is due to the diffusion of titanium in the cobalt matrix, promoted by high temperatures [9]. The solution found for this problem was the application of hard and self-lubricating coating on the rods. The manufacturer, Palbit, made a PVD nano composite coating with HiPIMS technology of TiAlSiN with 3 µm thickness. This coating reduces the coefficient of friction between the surfaces [10] and prevents the diffusion between the titanium and the cobalt matrix of the tungsten carbide [11]. After the application of this coating, the fracturing of the compression rods did not occur again.

Testing in high temperature conditions requires the use of an electric furnace that

surrounds the compression zone. This constraint led to the production of two distinct sets of incident and transmitter bars.

The first set, with the carbide compression rod observable in figure 3(a), also has threaded ends, allowing the installation of inductive position sensors, and has compression rods with a protruding length of 10 mm; this is the preferred set for carrying out tests at room temperature, as the reduced protruding length of the compression rods also reduces the risk of fracture.

The second set of compression rods has a protruding length of 80 mm, as shown in figure 3(b), so that they can be accommodated inside the electric furnace during the tests; this set is only used when carrying out high temperature tests, as there is a greater risk of fracture of the carbide rods due to their slenderness. In this case, as the inductive position sensors cannot be installed, an alternative system for measuring displacement using sliding potentiometers has been developed.

(a) (b)

Figure 3 - (a) 10 mm carbide compression rod for room temperature testing and (b) 80 mm carbide compression rod for high temperature use.

Energy Dissipation Components

The remaining energy produced by the impact tests in severe conditions was dissipated by two mechanisms: an energy dissipating block and a damping system. Both components had a reducing effect on the intensity of the pressure wave that is reflected by the end of the transmitter bar.

The block, made of steel with a mass of 25 kg, is in direct contact with the end of the transmitter bar, absorbing part of the energy from the impact test. The introduction of the damping system, consisting of two dampers with a load of 80 N fixed to the transmitter bar and the linear bushing bearing, reduces the intensity of its rebound when energy is transferred to the block.

Pneumatic Cannon

The installation of a pneumatic cannon as the propulsion system for the projectile allowed the performance of very high strain-rate tests.

This device, assembled in the right side of the impact bench as seen on figure 4, developed by Afonso Gregório (2017), is composed of a pressure chamber and a barrel that guides the projectile. The pressurized air in the pressure chamber drains into the pipe with the activation of a quick exhaust valve, propelling the projectile up to ballistic speeds above 100 m/s.

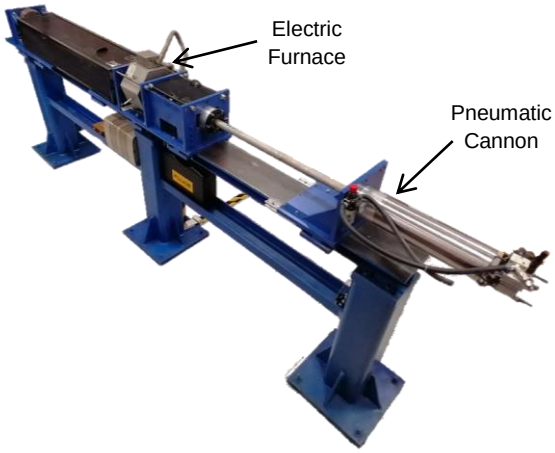

Figure 4 - Fully assembled impact bench in the high strain-rate and high temperature configuration.

Since the tank has a constant volume, the stored energy is exclusively a function of pressure, which can be modified through a pressure regulating valve installed in the device, this energy being transferred to the projectile. The projectile will acquire more speed the smaller the mass. That said, there is a set of projectiles with different masses, ranging from 250g and 3000g, thus allowing the use of a wide range of speeds.

Hydraulic actuator

The quasi-static compression tests were performed using a hydraulic actuator. This actuator was installed in the support structure and, when activated, pushes the incident bar, compressing the specimen.

Electric Furnace

As referred previously, in order to carry out the uniaxial compression tests at high temperatures, an electric furnace was installed in the test area, surrounding the compression rods, as seen in figure 4. This furnace consists of a chamber lined with refractory material where the electric heating

resistors are located, with the particularity of having a through hole in the side. This equipment was equipped with a set of guides, similar to a drawer, facilitating its assembly and disassembly.

The temperature measurement was performed in three different ways: with a thermocouple probe, temperature indicator pens and an infrared thermometer. Due to the reduced mass of the specimen, it was assumed that its temperature would be approximately the same as that of the compression rods. To facilitate the reading of the temperature on the rods, they were covered with a thin layer of black heat resistant silicone, with the exception of the compression plates, thus avoiding the reflection of the laser of the infrared thermometer and, due to the roughness of this layer, allow the indicator pens to paint the surface more easily.

Cryogenic Chamber

A cryogenic chamber, made of expanded polystyrene (EPS), was installed in a similar fashion as the furnace. This chamber could be filled with liquid nitrogen, effectively lowering the temperature of the specimen. The control of the temperature was done by adjusting the level of liquid and using the infrared thermometer.

Inductive Position Sensors

The inductive sensors are based on the principle of electromagnetic induction between coils. The electric current on one coil generates an electromagnetic field that will induce an electric current on the opposite coil. The distance between coils varies the induced electric current. Based on this concept, and by maintaining a constant voltage in the emitter coil, it is possible to determine the distance between coils through the voltage measured in the receiving coil.

The sensors were glued with epoxy resin to manufactured threaded adapters, and were installed on the previously threaded ends of the incident and transmitter bars.

The emitting coil was connected to a function generator. Since the signal sent by the function generator is an alternating current (AC) signal and the data acquisition board receives only direct current (DC) signals, it is necessary to use a rectifier bridge to translate the signal. Initially, the signal rectifier consisted of a rectifier bridge with 4 semiconductor silicon diodes, which transforms the signal, and a 1 nF capacitor at the output that smooths the signal. The use of this rectifier was interrupted due to the slow response incompatible with the performance of tests at high speed, caused by the capacitor. A commercial MB6M bridge rectifier, equipped with a 13 pF capacitor was installed. The response time improved, requiring only a minor temporal adjustment during the data post processing.

Sliding Potentiometer Sensors

The electric furnace installed in the test area prevents the use of the inductive sensors previously described. An alternative solution was developed using linear sliding potentiometers. The assembly of these devices was made taking advantage of the structure of the linear ball bearings that support the transmitter and incident bars. As can be seen in figure 5, an aluminium alloy plate was screwed to the ball bearing structure, allowing the potentiometer to be fixed, making its tab fit into a previously opened slot on the bar. Epoxy resin was then added to this connection between the potentiometer tab and the bar to prevent it from being released due to the violence of impacts.

A total of 3 potentiometers were installed: 1 on the incident bar and 2 on the transmitter bar allowing an indirect measure of the distance between compression plates.

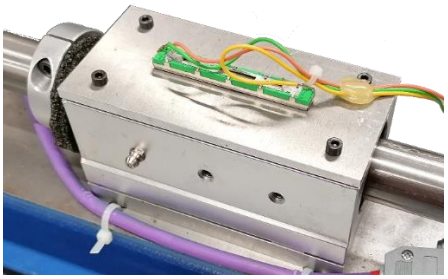

Figure 5 - Sliding potentiometer assembly in the linear ball bearing structure.

The potentiometers are supplied with a voltage of 5 V via DC power supply. The movement of the tab of the potentiometer varies the resistance, changing the value of the voltage registered in the output.

The calibration curve of the potentiometer is obtained using the calibrated specimens.

Load Sensor

The load is monitored by a load cell, a Wheatstone bridge strain gauge circuit, installed in the transmitter bars (figure 6). When the load cell is subjected to a certain load, the strain gauges' resistance changes, which in turn allows the calculation of the force exerted.

Figure 6 - Load cell installed in one of the transmitter bars.

The voltage value sent by the load cell is very low. A VISHAY 2310B signal conditioning and amplification system was connected to amplify the signal. The amplifier was set to a gain of 500, with a maximum excitation value of 10V.

The load cell calibration curve has been obtained using a commercial load cell.

Data Post-Processing

The construction of the equipment and the performance of compression tests are only the first steps needed to obtain valid results. The transformation of electrical signals, recorded by the instrumentation, into the intended physical values is not always direct; therefore, a careful processing of the data obtained is necessary.

To make this processing as fast and standardized as possible, a spreadsheet was created in the Excel software allowing the analysis and processing of the recorded data, from the electrical signals to the final stress-strain curves of the tested specimens.

Essentially, the data needed to obtain the values of stress and strain at each instant of compression of the cylindrical specimen are: its instant height, given by the distance between compression plates; the applied load, given by the load cell signal and the initial height and diameter of the specimen.

The different configurations of the equipment imply different data processing. In the case of quasi-static compression tests at room temperature, using the bars equipped with inductive sensors, the data processing is straight-forward, as this type of sensors give the distance between compression plates directly, only needing a slight time adjustment and signal smoothing.

The analysis of the equipment's behaviour during quasi-static compression tests, at high temperature, revealed that the elastic deformation of the transmitter bar caused the displacement obtained from the potentiometer installed in the incident bar to not correspond to the real distance between compression plates. The strategy of the analysis for this type of test was to perform an empty compression test, in which the relationship between the applied load and the displacement of the potentiometer in the incident bar is obtained; this relationship allows to obtain a factor that corrects the displacement according to the applied load, eliminating the contribution of the elasticity of the bars and the equipment.

The data obtained in the impact tests, at high strain-rate and temperature, could not be treated using the strategy described before, since the dynamic behaviour of the equipment at high speeds proved to be difficult to analyse and predict.

Firstly, the signal from the load cell has a characteristic signature. It was determined that this signature came from the reflection of the pressure wave in the transmitter bar. When it reaches the end of the bar, reflects and passes again in the load cell, leaving this bar in a state of vibration; knowing that the speed of sound in titanium is approximately 6000 m/s, the instant in which this signature begins corresponds to the time that the pressure wave takes to travel the distance between the load cell and the end of the bar and return, about 0.3 ms. The application of a Fourier filter targeted the characteristic frequency of this noise, mitigating its influence on the signal.

Secondly, the displacement correction using the load recorded during high speed and high temperature impact tests resulted below par. The installation of the two potentiometers in the transmitter bar allowed a correction taking into account their displacement during the impact test. It was possible to extrapolate the displacement of the compression plates by mathematically relating the three potentiometers.

4. Experimental Results

The first phase of the experimental plan consists in carrying out the validation of the equipment. For this purpose, cylindrical 6x6 mm specimens of aluminium alloy AA1050-O (99.5% wt.), annealed to 450ºC and cooled in air, were used, intending to reproduce the results obtained in the study by Alcino Reis (2016) regarding quasi-static tests, and the results published by Tiago dos Santos et al. (2017) regarding the impact tests.

In a second phase, in order to progressively test the equipment's capabilities, it was decided to carry out tests on two materials vastly used in engineering: AA 5083-H111 aluminium alloy and AISI 1045 steel.

In the third and last phase of tests, maraging 300 steel test pieces were tested, this being the challenge proposed for the developed test equipment. The specimens obtained have two distinct origins: a conventional commercial maraging 300 rod and a component produced in maraging 300 by Selective Laser Melting (SLM). All specimens are cylindrical and 4x4 mm.

Due to the characteristics of the SLM additive manufacturing process, the maraging 300 specimens obtained from the component produced by this method were divided into two different types, vertical and horizontal, depending on the orientation of the metal layers.

Validation

For the quasi-static validation, the bars with the inductive position sensors were mounted. This configuration is the one that allows greater accuracy in the results obtained since the sensors are mounted directly on the compression plates and are not sensitive to any external interference to the test, such as the elastic deformation of the test machine. Figure 7 shows the curve corresponding to the average of 3 tests performed compared with the curve obtained by Alcino Reis (2016). It is observed that the results overlap, showing good agreement between the plastic flow curves, allowing the validation of the test equipment in this configuration.

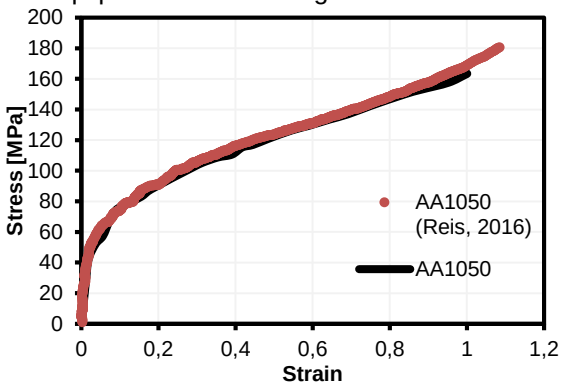

Figure 7 - Comparison of quasi-static stress-strain curves of AA1050-O obtained in this study against the ones obtained by Alcino Reis (2016)

In order to assess whether the sliding potentiometer sensors configuration with the electric furnace installed could produce valid results an attempt was made to reproduce the work of dos Santos et al. (2017) by performing tests on an AA1050 alloy at the same strain-rate. Based on the information from the calibration curves obtained by David Campos (2020) and through the selection of a projectile of adequate mass, it was possible to perform 3 tests at a strain-rate with an average profile of 1500 s^{-1}. Shown in figure 8 are the average stress-strain curve of the 3 tests, as well as the curve obtained by dos Santos et al. (2017). It is possible to observe a correspondence between both plastic flow curves, graphically represented by their overlap. This result makes it possible to validate the necessary configuration when using the furnace for temperature tests as well as the data processing procedure followed.

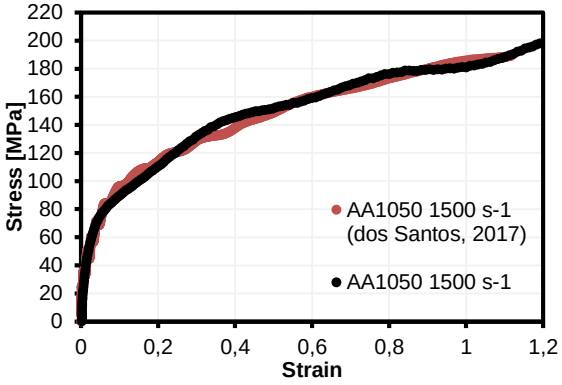

Figure 8 - Comparison of dynamic (1500s^{-1}) stress-strain curves of AA1050-O obtained in this study against the ones obtained by Tiago dos Santos (2016)

AA 5083-H111

The stress-strain curves obtained from the quasi-static compression tests, performed at variable temperatures, observed in figure 9, reveal a progressive softening of the material with the increase of temperature. A reduction in the flow stress of around 5% and 15% can be quantified, at a temperature of 50ºC and 100ºC, respectively, when compared to the flow curve at 25ºC, as well as an increase of 10% and 14% for -50ºC and 70ºC. An increase in the flow stress with the deformation also occurs, indicating the work hardening of the material that happens regardless of the temperature.

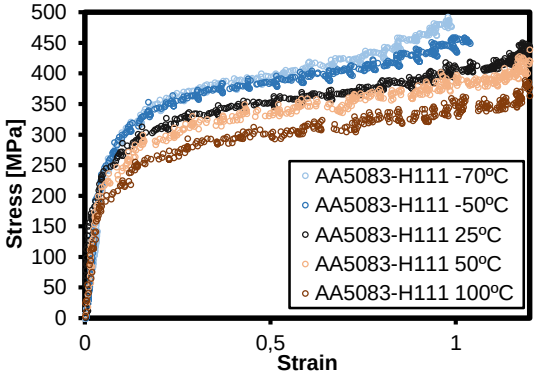

Figure 9 - Quasi-static compression stress-strain curves of AA 5083-H111 at various temperatures.

This aluminium alloy, AA 5083-H111, has good mechanical properties compared to other aluminium alloys typically used, except aluminium alloys for aerospace applications, but using it in operating conditions above 65ºC is not recommended. One of the reasons for this manufacturer indication may be the fact that the mechanical strength reduces dramatically above that temperature, which is particularly visible in the impact stress-strain curves in figure 10, at a strain-rate of 3000 s^{-1}. The reduction in yield stress compared to the test at 25ºC is in the order of 10% and 30%, for temperatures of 50ºC and 100ºC respectively.

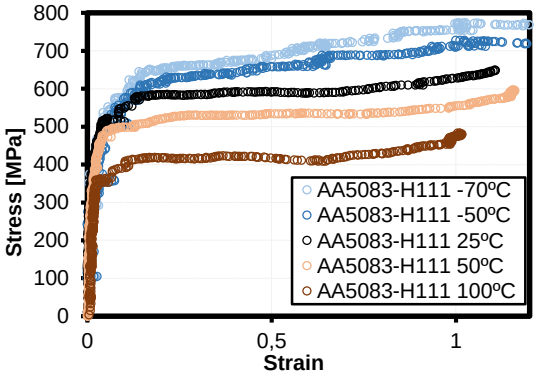

Figure 10 - Dynamic compression stress-strain curves of AA 5083-H111 at 3000 s^{-1} and various temperatures.

Maraging 300

In a first analysis, compression tests were carried out, always at room temperature, varying only the deformation rate, from the quasi-static regime to strain-rates of 6000 s^{-1}. The plastic flow curves of the material make it possible to compare the influence of the strain-rate on each material and also to compare the behaviour of the conventional material against the one produced by SLM, and, in addition, whether the orientation of the deposition layers of the metal by additive manufacturing, have influence in its behaviour when subjected to compressive loads.

The graph in figure 11 shows the evolution of the flow curve for conventional maraging 300 specimens. In the quasi-static test curve, after a yield stress of 1150 MPa is exceeded, a slight negative evolution of the flow stress can be observed. Only after an extension around 0.3 the work hardening phenomenon starts. In dynamic tests this is even more pronounced. This stress saturation behaviour of plastic flow might be characteristic of maraging, as even in the SLM samples display this behaviour.

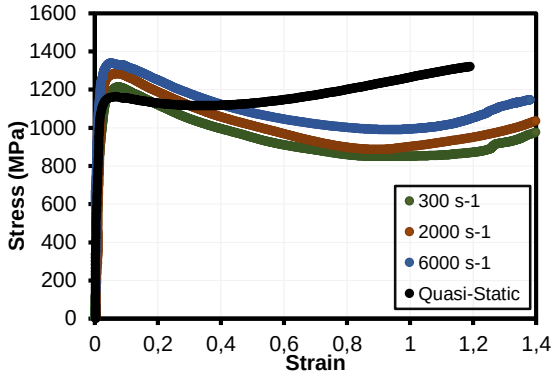

Figure 11 – Stress-strain curves of conventional maraging 300 compression at different strain-rates.

The SLM maraging 300 specimens show an increase in flow stress of approximately 10% in the horizontal case and 7% in the vertical case, compared to the conventional maraging 300. This might be due to the aging of the metal during the manufacturing process. The fusion of the successive layers during their deposition causes the metal to maintain a temperature conducive to its aging, slightly increasing the mechanical resistance.

Between specimens with layers of material vertically and horizontally, the difference in flow stress is not significant, the horizontal maraging 300 specimens show a higher flow stress in the order of 3%. The height of the layers, although it was not possible to measure them, would be around 30 µm to 50 µm, characteristic of the SLM process, and could be the cause of this apparently isotropic behaviour.

The influence of temperature was first studied in a quasi-static regime. The graph in figure 12 shows the flow curves of quasi-static tests performed at variable temperature in the horizontal maraging 300 specimens. It is possible to observe a reduction in the flow stress with increasing temperature, which would be predictable taking into account the typical behaviour of metals with temperature rise. The same was verified for the conventional maraging 300.

All the maraging 300 specimens show a reduction of about 15% in the flow stress at a temperature of 200ºC, compared to 25ºC, but present a negligible difference in relation to 370ºC. At 600ºC, the horizontal maraging 300 suffers a reduction in flow stress of 30%, but from an extension of 0.5 this stress has a higher evolution than that registered at lower temperatures.

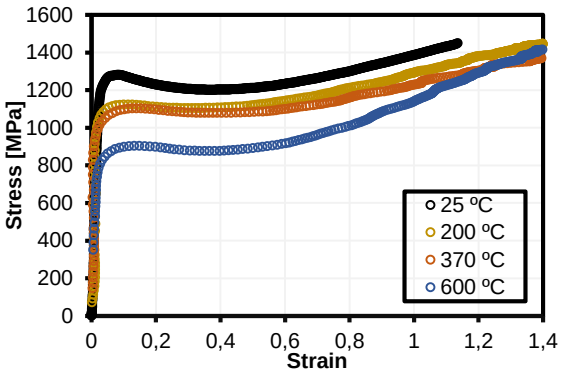

Figure 12 - Stress-strain curves of horizontal SLM maraging 300 quasi-static compression at different temperatures.

As shown in the graph of figure 13, the introduction of high strain-rates to high temperature compression tests has brought unexpected results from the point of view of the material's behaviour. This graph includes the impact test with a strain rate of 2000 s^{-1} at room temperature (25ºC) previously analysed, in order to be able to analyse the change in the evolution of the material flow stress.

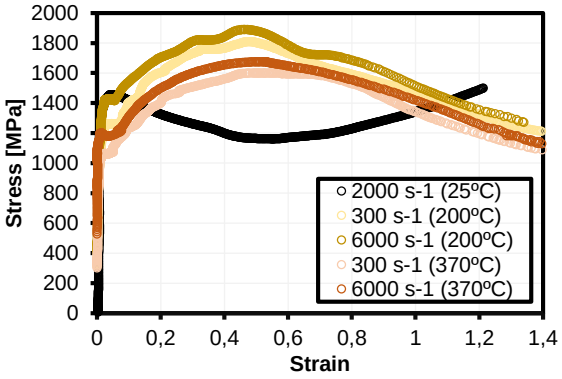

Figure 13 - Stress-strain curves of horizontal SLM maraging 300 compression at different temperatures and strain-rates.

In both the conventional maraging 300 and horizontal maraging 300, the increase in temperature causes the elimination of the initial softening of the flow curve causing, up to extensions of approximately 0.5, a positive evolution of the flow stress, followed by a drastic softening.

This material's mechanical behaviour could not be modelled by the constitutive models presented, as none of them predict such a softening with increasing strain-rates or hardening with increasing temperatures.

5. Model Calibration

The data obtained experimentally from the AA5083-H111 alloy and AISI 1045 steel specimens was used to obtain the calibration parameters of an adaptation of the Silva model. Since the Silva model does not account for the temperature factor, and the Johnson-Cook model does not model correctly the behaviour of the materials observed experimentally, another term was added to the equation of Silva's empirical model (eq. 3) for each material: Eq. 6 for AA 5083-H111 and eq. 7 for AA 1045.

$$[1 - E \cdot ln(T) \cdot T^{p}/F] \quad (6)$$

$$[1 - ((E/1 - T) + F)^{p}] \quad (7)$$

Table 1 – Parameters for AA 5083-H111 constitutive model.

A	B	C	D	E	F	m	n	p
-0,9719	-329,9679	-85,9349	31,0571	4,1701	0,0211	-0,00456	0,005	-0,6548

Table 2 - Parameters for AISI 1045 constitutive model.

A	B	C	D	E	F	m	n	p
-0,2496	777,0328	155,1713	497,3815	66,0259	1,0243	-0,0936	0,1817	13,6705

As can be seen in the graph in figure 14, the AA5083-H111 model has a good correspondence to the flow curve in quasi-static regime (black and green curves), but not so much in the dynamic regime (red and blue).

For the AA 1045 steel, the graph in figure 15 shows a good correspondence for the reference quasi-static test at room temperature (blue) but falling short in modelling the almost rigid-perfectly plastic behaviour of the 400ºC quasi-static test (yellow), as well as the 200ºC quasi-static test.

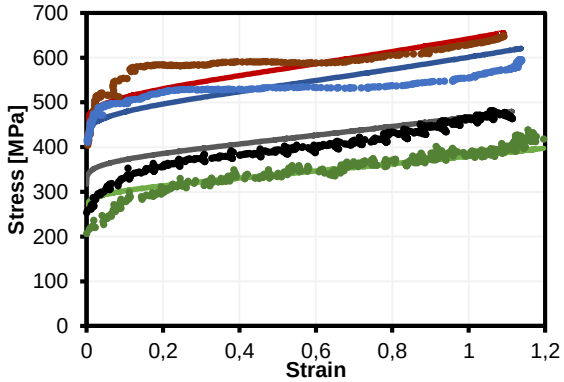

Figure 14 - Adapted Silva model adjusted to the AA5083-H111 stress-strain curves.

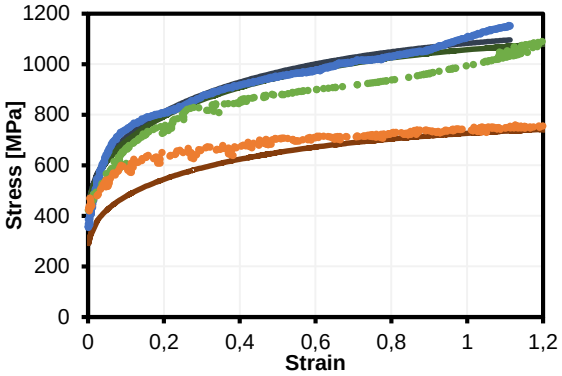

Figure 15 - Adapted Silva model adjusted to the AISI1045 stress-strain curves

6. Conclusions

The development of the experimental equipment and the successful accomplishment of tests in the proposed conditions allow to conclude that the main objectives of this work were fulfilled. Compression tests were carried out from the quasi-static regime up to deformation speeds in the order of 6000 s^{-1} at high and low temperature conditions, which represented an advance in the testing capabilities currently available at Instituto Superior Técnico.

The application of the constitutive models to the tested materials did not have the intended success. The closed structure of the phenomenological model only allows calibration parameters to be obtained for the conditions in which they were developed, falling short of what is expected in situations where, for example, new materials are tested under unusual conditions. In the case of maraging, the applied models do not have the capacity to model the unusual behaviour that it presents.

High speed impact tests are characterized by the production of vibrations that interfere with the signals registered by the sensors. In this specific case, the pressure wave reflected at the end of the transmitter bar caused a typical signature on the signal acquired by the load cell, and there was a need to develop mathematical strategies to resolve this situation. The use of a transmitter bar with enough length, to the point that the reflected wave has no influence on the signal, would be an improvement that would make it easier to treat the data originated by the impact tests.

The versatility of the developed equipment is one of its strengths; the ease of installation and adaptation of components that allow testing in different conditions, as was the case with the electric furnace, creating new challenges and opening the door to further improvements and studies.

References

[1] C. M. . Silva, P. A. R. Rosa, e P. A. F. Martins, «Innovative Testing Machines and Methodologies for the Mechanical Characterization of Materials», *Exp. Tech.*, 2014.

[2] M. Negahban, *The Mechanical and Thermodynamical Theory of Plasticity*. 2012.

[3] P. Perzyna, «Fundamental Problems in Viscoplasticity», *Adv. Appl. Mech.*, vol. 9, n. C, pp. 243–377, 1966.

[4] R. M. Jones, *Deformation Theory of Plasticity*. Blacksburg, Virginia: Bull Ridge Publishing, 2009.

[5] G. R. Johnson e W. H. Cook, «Fracture Characteristics of Three Metals Subjected to Various Strains, Strain rates, Temperatures and Pressures», *Eng. Fract. Mech.*, vol. 21, n. 1, pp. 31–48, 1985.

[6] C. Silva, «Caracterização Mecânica e à fratura de materiais aplicada a processos de deformação plástica e corte», PhD in Mechanical Engineering, Instituto Superior Técnico, Universidade Técnica de Lisboa, 2013.

[7] K. T. Ramesh, «High Strain Rate», em *Handbook of Experimental Solid Mechanics*, 2008, p. 874.

[8] T. L. M. C. A. Pires, «Barra de Pressão de Hopkinson», Escola Superior Náutica Infante D. Henrique, 2016.

[9] M. Chandrashekar e K. V. Sreenivasa Prasad, «The Effect of Cobalt on Wear behavior of Cemented Carbide cutting tools for machining of Titanium alloy», *Mater. Today Proc.*, vol. 5, n. 2, pp. 7678–7684, 2018.

[10] N. He, H. Li, L. Ji, X. Liu, H. Zhou, e J. Chen, «High temperature tribological properties of TiAlSiN coatings produced by hybrid PVD technology», *Tribol. Int.*, vol. 98, pp. 133–143, 2016.

[11] G. Bilger, T. Voss, T. Schlenker, e A. Strohm, «High-temperature diffusion barriers from Si-rich silicon-nitride», *Surf. Interface Anal.*, n. 38, pp. 1687–1691, 2006.